Journal of Physics: Conference Series **200** (2010) 012114 doi:10.1088/1742-6596/200/1/012114

Transport and magnetic properties of electron-doped manganites $CaMn_{1-x}Sb_xO_3$

Y Murano[1], M Matsukawa[1], S Kobayashi[1], S Nimori[2] and R Suryanarayanan[3]

[1] Department of Materials Science and Engineering, Iwate University, Morioka 020-8551, Japan
[2] National Institute for Materials Science, Tsukuba 305-0047 ,Japan
[3] Laboratoire de Physico-Chimie de L'Etat Solide, CNRS,UMR8182 Universite Paris-Sud, 91405 Orsay, France

E-mail: [1] matsukawa@iwate-u.ac.jp

Abstract. We report transport and magnetic properties of electron-doped manganites $CaMn_{1-x}Sb_xO_3$. The substitution of Sb^{5+} ion for Mn $^{4+}$site of the parent matrix causes one-electron doping with the chemical formula $CaMn^{4+}_{1-2x}Mn^{3+}_xSb^{5+}_xO_3$. Single phase samples ($x$=0.02, 0.05, 0.08 and 0.1) are prepared with a solid-state reaction method. Upon increasing the doping level of Sb, the resistivity is suppressed at high temperatures, accompanied by carrier doping. However, it is strongly enhanced at low temperatures because the presence of the Sb ion prevents moving of carriers on the MnO network. Seebeck coefficient of the samples studied shows a negative value over a whole range of temperatures, indicating the electron doping. An anomalous diamagnetic behavior is observed at x=0.02 0.05 and 0.08, as it has been reported in the V doped manganites. These findings are close to the variation of e_g orbital state due to the local lattice distortion associated with the Sb doping.

1. Introduction

Manganese oxides with perovskite structure have been extensively investigated since the discovery of colossal magnetoresistance (CMR) effect. The field induced insulator to metal transition and its associated CMR effect are well explained on the basis of the double exchange (DE) model between Mn^{3+} and Mn^{4+} ions. Furthermore, the phase separation model, where the ferromagnetic (FM) metallic and antiferromagnetic (AFM) insulating clusters of competing electronic phases coexist, strongly supports experimental studies of manganites. The static Jahn-Teller (JT) effect of Mn^{3+} ions plays a crucial role in the physics of manganites. In this work, we concentrate on the effect of Sb substitution on transports and magnetic properties of electron-doped manganites $CaMn_{1-x}Sb_xO_3$. It is shown that substituting of the Mn site of $CaMnO_3$ with pentavalent ions creates Mn^{3+} ions i.e.,electrons leading to the CMR effect[1]. It thus is interesting to examine the physical properties of the Mn-site substituted compositions for our understanding of electronic phase diagram of electron-doped manganites. Recently, an anomalously diamagnetic behavior in V^{5+} doped $CaMnO_3$ manganites has been reported[2].

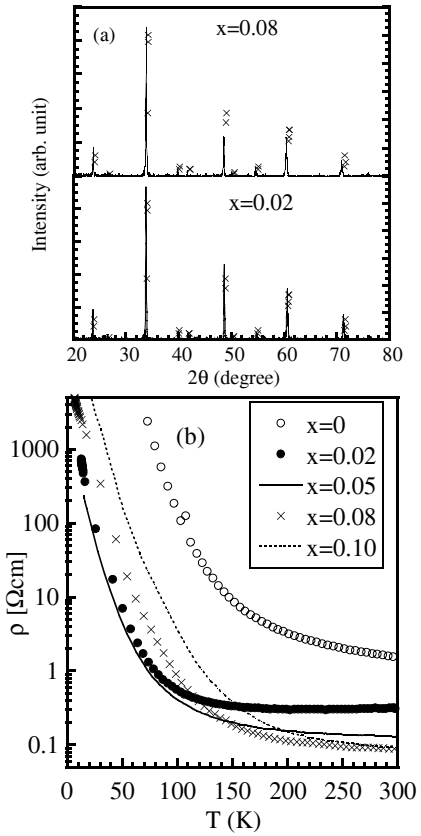

Figure 1. (a) X-ray diffraction data of the x=0.02 and 0.08 samples at room temperature. The symbols (×) indicate ideal peak values of the parent $CaMnO_3$ (orthorhombic space group *Pnma*). (b)Temperature variation of electrical resistivity for the $CaMn_{1-x}Sb_xO_3$ system (x=0.02, 0.05, 0.08 and 0.1). For comparison, the ρ data of the x=0 parent compound are presented.

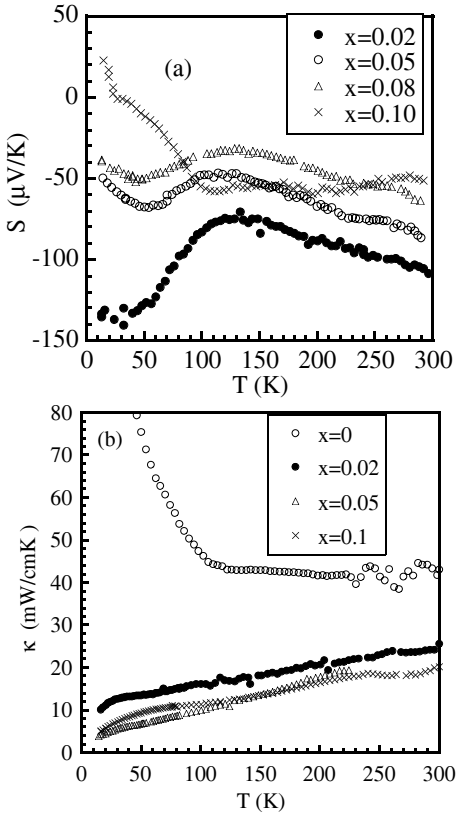

Figure 2. (a)Temperature variation of Seebeck coefficient S for the $CaMn_{1-x}Sb_xO_3$ system (x=0.02, 0.05, 0.08 and 0.1).(b) Thermal conductivity κ of $CaMn_{1-x}Sb_xO_3$ (x=0.02, 0.05 and 0.1). For comparison, the κ data of the parent compound $CaMnO_3$ are presented.

2. Experiment

Polycrystalline samples of $CaMn_{1-x}Sb_xO_3$ (x=0.02, 0.05, 0.08 and 0.1) were prepared with a solid-state reaction method. The stoichiometric mixtures of $CaCO_3$,Mn_3O_4 and Sb_2O_3 high purity powders were calcined in air at 1000 °C for 24 h. The products were then ground and pressed into cylindrical pellets. The pellets were finally sintered at 1400 $\sim$ 1450 °C for 12 h. X-ray diffraction data revealed that all samples are almost single phase with orthorhombic structures (*Pnma*)(Fig.1(a)). The lattice parameters of the x=0.08 sample are a = 5.326 Å, b = 7.512 Åand c = 5.310 Å, which is fairly agreement with a previous work[3]. The cell parameters and unit cell volume are elongated upon increasing the Sb doping because the ion radius of Sb^{5+} (0.61Å) is greater than the value of Mn^{4+} (0.54Å). In addition, the Mn^{4+} ions are replaced by Mn^{3+} ions (0.645Å) with one extra electron, which contributes to the enhanced cell volume. The electrical resistivity was measured with a four-probe method. Seebeck coefficient was determined from both measurements of a thermoelectric voltage and temperature difference

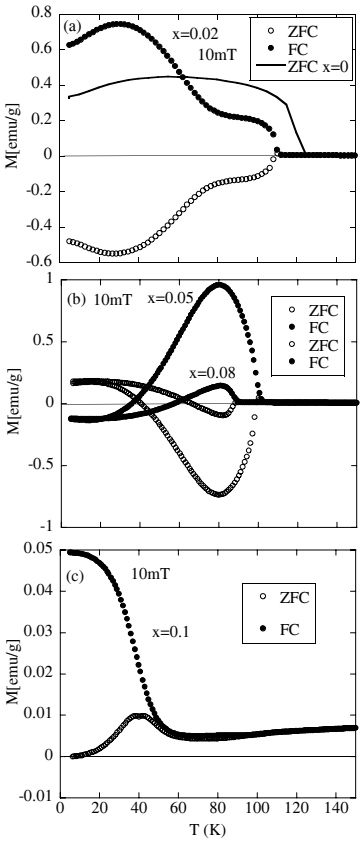

Figure 3. Temperature dependence of zero field cooled and field cooled magnetization of the Sb substituted $CaMn_{1-x}Sb_xO_3$ measured under an applied magnetic field of 10 mT (a) x=0.02, (b) x=0.05 and 0.08, (c) x=0.1. For comparison, the ZFC data of the parent sample are given in (a).

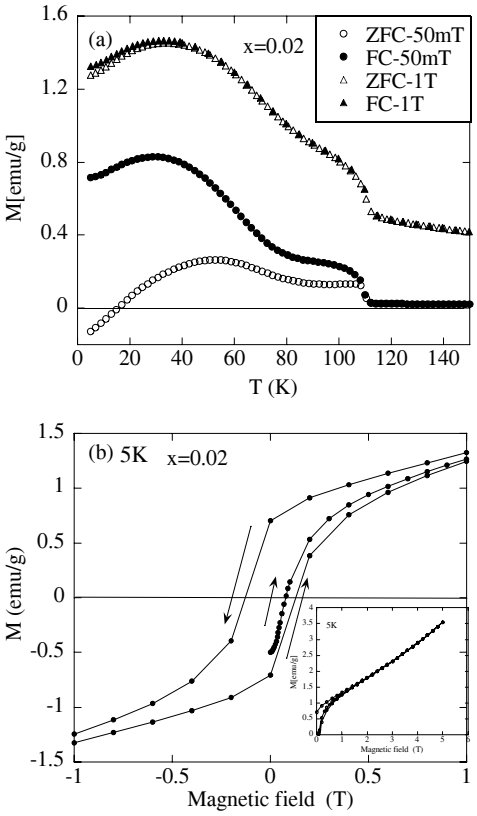

Figure 4. (a)Magnetization curves of the x=0.02 sample at applied fields of 50 mT and 1T. (b) Magnetic field dependence of the ZFC magnetization of the x=0.02 sample at 5 K. The inset of (b) shows the M data up to 5T.

along the longitudinal direction of the measured sample. The thermal conductivity was collected with a conventional heat flow method. The magnetization measurement was carried out using commercial SQUID magnetometers both at Iwate Univ. and National Institute for Materials Science.

3. Results and discussion

The temperature variation of electrical resistivity ρ for the $CaMn_{1-x}Sb_xO_3$ system is shown in Fig.1(b) as a function of the Sb content. The Sb substitution for Mn site up to x=0.05 gives rise to a substantial decrease in ρ at high temperatures, indicating the carrier doping into Mn-site. For further substitution of Sb (x=0.08 and 0.1), the magnitude of ρ at room temperatures is not changed. All samples exhibit semi conducting behaviors upon decreasing temperatures. On the other hand, the magnitude of the resistivity of the x=0.08 and 0.1 is enhanced at lower temperatures since the higher doping of Sb ion breaks some of conduction paths along the Mn-O network, resulting in reinforcing carrier localization. Next, Seebeck coefficient S is in magnitude suppressed upon increasing Sb doping as shown in Fig.2(a). For all samples studied, S shows a

negative value over a wide range of temperatures, which strongly suggests electron doping into the parent matrix. In the case of the substitution of Sb^{5+} ion for Mn^{4+} site, the Mn^{4+} ions are replaced by Mn^{3+} ions with one extra electron. For lower doped samples(x=0.02 and 0.05), the local maximum observed in S is located near the magnetic transition temperature as mentioned below. The light doping of Sb^{5+} strongly suppresses the magnitude of thermal conductivity from 80 mW/cmK (50K) at the pure x=0 sample down to 14 mW/cmK at x=0.02 (Fig.2(b)). Let us show in Fig. 3 the zero-field cooled (ZFC) and field cooled (FC) magnetization data of the Sb substituted $CaMn_{1-x}Sb_xO_3$ measured under an applied magnetic field of 10 mT. First of all, anomalously diamagnetic behavior appears below the magnetic transition temperature T_m=110 K for x=0.02, as it has been reported in the V doped $CaMn_{1-x}V_xO_3$manganites [2]. The ZFC curve seems to be a mirror image of the FC curve with respect to the horizontal axis. For x=0.05, the ZFC-M(T) curve starts from its positive value, then shows a monotonic decrease upon increasing T,and finally reaches a negative minimum around 80 K. The negative magnetization is limited between the intermediate and magnetic transition temperatures. We notice similar characters in the magnetization data of both the x=0.05 and 0.08 samples. However, at highly Sb doped sample(x=0.1), such negative magnetization vanishes and instead a large divergence between ZFC and FC curves appears at low temperatures, suggesting spin-glass like magnetic state. The magnetic transition temperature is suppressed from 125 K at x=0 down to 50 K x=0.1 due to the Sb doping because the Sb^{5+} ion is non magnetic one with the closed shell of $4d^{10}$. We note that the parent composition is a G-type AFM insulating state. Next, we examine the magnetic properties of the x=0.02 sample in different fields of 50 mT and 1 T as shown in Fig.4(a). In a field of 50 mT, the negative magnetization disappears above 10 K. Moreover, in an application of relatively high field of 1T, the diamagnetism is fully destroyed and magnetic hysteresis also vanishes. Figure 4(b) displays the $M(H)$ loop of the x=0.02 sample measured at 5 K. The $M(H)$ data with a small hysteresis do not saturate even at 5 T and rises linearly with increasing H as shown in the inset of Fig.4(b), indicating the AFM matrix with small FM phase. The initial $M(H)$ curve recorded at 5 K is changed from its negative to positive sign when the applied field exceeds 0.1 T. The Sb^{5+} doping removes the Mn^{4+} ion and instead produces the Mn^{3+} ion for Mn sites which is the Jahn-Teller active ion with one e_g-electron. It is believed that the local lattice distortion due to JT effect causes phonon scattering, which is close to the depressed thermal conduction[4]. In addition, the lattice deformation due to the Sb doping with its larger ion radius affects the neighboring $Mn^{3+}O_6$ octahedron, resulting in some variation of the orbital-state of e_g-electron through the local JT effect. We suppose that the orbital-spin coupling at $Mn^{3+}O_6$ probably gives rise to a canted spin alignment in a direction opposite to the applied field, leading to negative magnetization curves at low fields. In YVO_3 with a distorted perovskite structure, temperature-induced magnetization reversals observed are explained on the basis of the Dzyaloshinsky-Moriya interaction which prefers canted spin arrangements[5]. In summary, we have investigated the effect of Sb substitution on electrical and thermal transports, and magnetic properties of electron-doped manganites $CaMn_{1-x}Sb_xO_3$.
This work was supported by a Grant-in-Aid for Scientific Research from Japan Society of the Promotion of Science.

4. References

[1] Raveau B, Zhao Y M ,Martin C, Hervieu M, and Maignan A 2000 *J. Solid State Chem.* **149** 203.
[2] Ang R, Sun Y P ,Ma Y Q, Zhao B C, Zhu X B and Song W H 2006 *J.Appl.Phys.* **100** 063902.
[3] Poltavets Victor, Vidyasagar K and Jansen M 2004 *J. Solid State Chem.* **177** 1285.
[4] Matsukawa M, Narita M, Nishimura T,Yoshizawa M, Apostu M, Suryanarayanan R, Revcolevschi A and Itoh K Kobayashi N 2003 *Phys.Rev.* B **67** 104433.
[5] Ren Y, Palstra T T M, Khomskii D I,Pellegrin E, Nugroho A A, Menovsky A A and Sawatzky G A 1998 *Nature* **396** 441.